

# Different roles of carbon and silicon interstitials in the interstitial-mediated boron diffusion in SiC

Michel Bockstedte, Alexander Mattausch, and Oleg Pankratov

*Lehrstuhl f. Theoretische Festkörperphysik, Universität Erlangen-Nürnberg, Staudtstr. 7B2, D-91058 Erlangen, Germany*

(Received 24 March 2004; revised manuscript received 18 May 2004; published 8 September 2004)

The interstitial and vacancy mediated boron diffusion in silicon carbide is investigated with an *ab initio* method. The boron interstitials in *p*-type and *n*-type materials are found to be far more mobile than the boron-vacancy complexes. A kick-out mechanism and an interstitialcy mechanism govern the diffusion in *p*-type/intrinsic and *n*-type material, respectively. A comparison of activation energies demonstrates that the equilibrium diffusion is dominated by the positive hexagonal interstitial for typical experimental conditions. The activation energy and the charge state is in agreement with experimental findings. The analysis of the kick-out reaction demonstrates that silicon and carbon interstitials have different effects on boron acceptors on the silicon and carbon sublattice ( $B_{Si}$  and  $B_C$ ). While silicon interstitials mediate the diffusion of both acceptors, carbon interstitials are only relevant for  $B_C$ . A larger kick-in barrier into silicon sites is found than into carbon sites. This implies a dominant formation of  $B_C$  in the extended diffusion tails of boron profiles. The stable boron complexes with carbon or boron interstitials are found that potentially reduce the boron diffusion. This and the characteristics of the kick-out mechanism facilitate an explanation of recent co-implantation experiments.

DOI: 10.1103/PhysRevB.70.115203

PACS number(s): 61.72.Ji, 66.30.Jt, 85.40.Ry

## I. INTRODUCTION

The dopant diffusion in semiconductors is a fundamental physical phenomenon. Substitutional dopants are *per se* immobile and need vacancies or interstitials as diffusion vehicles.<sup>1</sup> Uncovering of the dominant diffusion channels also has technological relevance. For example, implanted impurity profiles can be seriously affected by the transient enhanced impurity diffusion during the annealing. The means to control this effect is tightly related to the diffusion mechanism.

The boron diffusion in the wide band gap semiconductor silicon carbide is a rather complicated case. In the compound material, vacancies and interstitials of both chemical species can contribute to the diffusion. Boron is known to substitute for the silicon-site ( $B_{Si}$ ),<sup>2,3</sup> where it acts as a shallow acceptor. But it may also substitute for carbon ( $B_C$ ), as indicated by experiments<sup>4,5</sup> and predicted by theory,<sup>6,7</sup> and form a deep acceptor.

Early experiments<sup>8,9</sup> on the boron diffusion in SiC have been interpreted in terms of a vacancy-mediated diffusion. From the characteristic dependence of the boron diffusion on aluminum doping, Mokhov *et al.*<sup>9</sup> concluded that a positive boron-related defect mediates the diffusion. Yet, their model was challenged by recent coimplantation experiments<sup>10</sup> and by the detailed analysis of boron diffusion-profiles.<sup>11,12</sup> All these works favor a kick-out mechanism. In implantation experiments a transient enhanced boron diffusion was observed.<sup>10,13</sup> Laube *et al.*<sup>10</sup> were able to suppress the effect by a coimplantation of carbon, while a silicon coimplantation enhanced the diffusion. Their interpretation suggests a kick-out mechanism based on silicon interstitials, which is plausible if  $B_{Si}$  is the dominant boron defect. Also a retardation of the diffusion by carbon-related defects was postulated, in analogy with the case in silicon.

However, the boron diffusion may be even more complex. This is indicated by the observation of the boron-related D-center in annealed boron-implanted samples<sup>14,15</sup> and of the deep acceptor in samples doped by in-diffusing boron.<sup>9,16</sup> Gong *et al.*<sup>15</sup> and Gao *et al.*<sup>16</sup> suggested that these boron defects were located in the extended diffusion tails.

Theoretical investigations on the boron diffusion in SiC are sparse. *Ab initio* investigations<sup>7,17</sup> identified the dominant boron interstitial sites and boron-vacancy complexes for different doping conditions in 3C-SiC. Also the migration was investigated including the kick-out reaction of  $B_{Si}$  by a silicon interstitial.<sup>7</sup> The boron-interstitials in *p*-type material, i.e., a carbon-coordinated tetrahedral interstitial and a hexagonal interstitial, were found to migrate much faster than the boron-vacancy complexes. Later, *ab initio* molecular dynamics simulations<sup>18</sup> were conducted for the neutral hexagonal interstitial in 3C-SiC. In the simulation, a kick-out by a silicon interstitial initiated the boron migration. Rurali *et al.*<sup>18,19</sup> further analyzed a migration path of neutral hexagonal interstitial and also included charge state effects. Their simulation corroborates the relevance of the kick-out mechanism. This is an important point. For example, in silicon the boron diffusion was found to be dominated by an interstitialcy mechanism instead of the originally proposed kick-out mechanism.<sup>20-22</sup>

However, the present-day understanding of the boron diffusion is limited. In particular, the role of carbon and silicon interstitials in the kick-out mechanism and the effect of stable complexes of boron with interstitials have not been addressed to date. Also the boron migration in *n*-type material and the relevance of a vacancy-assisted mechanism demand further investigations.

In this paper we present an investigation of the boron diffusion by an *ab initio* method based on density functional theory. We investigate the kick-out reactions and small

boron-related interstitial clusters to understand their relevance for the boron-diffusion. Our analysis of the boron interstitial sites in 4H-SiC shows that the results for the cubic polytype are transferable to the hexagonal polytype. Therefore we conduct the computationally demanding investigation of migration or reaction paths in cubic SiC. We find that three distinct boron interstitials are relevant for the migration, namely, the tetrahedrally carbon-coordinated site ( $p^+$ -type), the hexagonal site ( $p$ -type and intrinsic), and the boron split interstitial at the silicon site ( $n$ -type). The dominant boron-vacancy complexes are the nearest-neighbor complex  $B_{Si}-V_C$  and the second-neighbor complex  $B_C-V_C$ . The activation energies of the corresponding diffusion channels determine their contribution to the equilibrium boron diffusion. A comparison of the calculated values demonstrates the dominance of the interstitial-mediated diffusion. The analysis of Fermi-level effects shows that the positive hexagonal boron interstitial explains the findings of Mokhov *et al.*<sup>9</sup> The calculated activation energy is in good agreement with the experimental value for the equilibrium diffusion.<sup>23</sup> Our investigation of the kick-out reactions shows that carbon and silicon interstitials have a different effect on the boron diffusion. While the silicon interstitials drive the kick-out of substitutional boron on both sublattices, the carbon interstitials only affect the migration of  $B_C$ . The kick-out barriers are typically low. We find substantially larger kick-in barriers, in particular for a kick-in to the silicon site. This means that predominantly  $B_C$  will form in the extended diffusion tails. Furthermore, stable boron-interstitial complexes are found. Such boron traps can result in a retardation of the diffusion. Traps formed by a carbon interstitial and  $B_{Si}$  and a boron-carbon pair residing at a hexagonal interstitial site may explain the slowing down of the boron diffusion upon carbon co-implantation. On the contrary, the only stable boron complex with a silicon interstitial that we found rather contributes to the diffusion. We also report a formation of a stable boron pair at a silicon site that may effect the diffusion at high boron concentrations.

The paper is organized as follows. In Sec. II we briefly outline the method. Our findings for the ground state configuration of boron interstitials in 3C- and 4H-SiC are discussed in Sec. III together with the corresponding migration mechanisms in 3C-SiC. An analysis of the reactions of  $B_{Si}$  and  $B_C$  with silicon and carbon interstitials is given in Sec. IV. We then turn to small stable boron complexes with interstitials, which may contribute to a retardation of the boron diffusion. The vacancy-mediated diffusion is analyzed in Sec. VI. In Sec. VII we apply the outlined mechanisms to the case of equilibrium diffusion and discuss the different effect of carbon and silicon interstitials on the annealing of implanted boron-profiles and on the situation in the extended diffusion tails. A summary concludes the paper.

## II. METHOD

The analysis of the boron diffusion was carried out by means of total energy calculations within the framework of density functional theory. We employed the plane-wave pseudopotential code FHI96SPIN<sup>24</sup> together with the local den-

sity approximation for the exchange-correlation energy functional. Optimized norm-conserving pseudopotentials of the Troullier-Martins type were generated with the help of the FHIPP package<sup>25</sup> that enable well converged calculations in a plane wave basis set with a cut-off energy of 30 Ry. Supercells with 64 lattice sites and a special  $\mathbf{k}$  point set<sup>26</sup> with eight  $\mathbf{k}$  points in the Brillouin zone ( $2 \times 2 \times 2$ -mesh) were used. The results for the boron interstitials and vacancy complexes were checked using a supercell with 216 lattice sites. Consistency checks for these defects in 4H-SiC were carried out in cells with 128 lattice sites.

We analyzed the electronic and structural properties of the defects. The concept of formation energy, as outlined, e.g., in Refs. 6 and 27, was employed to assess the energetics of charged defects and to determine the most relevant defect configurations for a given Fermi level  $\mu_F$ . The formation energy also contributes to the activation energy of the diffusion (cf. Sec. VII). For the sake of clarity we briefly outline the basic formulas. The formation energy of boron-related defects in a charge state  $q$  is given by

$$E_f = E_{f,0} - (n_{Si} - n_C)\Delta\mu_{Si} - n_B\Delta\mu_B + q\mu_F, \quad (1)$$

where  $n_B$ ,  $n_{Si}$ , and  $n_C$  denote the number of boron, silicon, and carbon atoms that comprise the defect in the supercell. The chemical potentials  $\Delta\mu_B$  and  $\Delta\mu_{Si}$  are defined relative to icosahedral boron<sup>28</sup> and crystalline silicon.  $E_{f,0}$  is obtained from the total energies of the defect cell and the reference crystals as  $E_{f,0} = E_{D,cell} - n_C E_{SiC} - (n_{Si} - n_C) E_{Si} - n_B E_{B_{12}} + qE_V$ , where  $E_V$  is the position of the valence band edge. The phase stability of SiC allows  $\Delta\mu_{Si}$  to vary within the bounds  $-H_{f,SiC} < \Delta\mu_{Si} < 0$ , where  $H_{f,SiC}$  is the heat of formation of SiC (cf. Ref. 27 for details). The upper (lower) bound corresponds to an excess of silicon (carbon), i.e., Si-rich (C-rich) conditions, and reflects the stoichiometry of the crystal. The Fermi level  $\mu_F$  is determined by the neutrality condition

$$\sum_i q_i c_i + N_C e^{-(E_{gap} - \mu_F)/k_B T} - N_V e^{-\mu_F/k_B T} = 0, \quad (2)$$

where the sum includes the concentration  $c_i$  of all defects and their charge states  $q_i$ .  $E_{gap}$  is the experimental band gap and  $N_C$  and  $N_V$  are the statistical weights of free electrons and holes.<sup>29</sup> The concentration  $c_i$  is given by  $c_i = c_s \exp(-E_f/k_B T)$ ,  $c_s$  is the concentration of lattice sites. The total boron concentration  $c_B$  is thus a function of  $\Delta\mu_B$ ,  $\Delta\mu_{Si}$ , and the temperature  $T$ . This relation is used to determine  $\Delta\mu_B$  for the comparison of calculated and experimental activation energies.

In the calculation of charged defects we apply the Makov and Payne correction<sup>30</sup> to remove the artificial Coulomb interactions. Calculated ionization levels indicate the range of  $\mu_F$  where a particular charge state of a defect is stable (or metastable). The analysis of the interstitial migration, the kick-out/kick-in reactions and the vacancy migration was conducted exclusively in 3C-SiC to keep the calculation tractable. We employ the ridge method of Ionova and Carter<sup>31</sup> to search for the saddle point on the potential energy surface between the initial and final site of a migration or kick-out/kick-in event. This search is conducted for all rel-

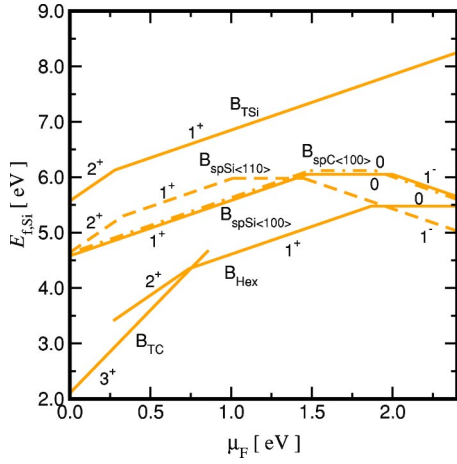


FIG. 1. Boron interstitials: formation energy for Si-rich conditions in 3C-SiC. Dashed or dash-dotted lines are used to distinguish the formation energy of  $B_{spSi\langle 110 \rangle}$  and  $B_{spC\langle 100 \rangle}$  from that of  $B_{spSi\langle 100 \rangle}$ , respectively. Charge states are indicated. The geometry of the most stable boron interstitials and the intermediate sites  $B_{spSi\langle 100 \rangle}$  and  $B_{spC\langle 100 \rangle}$  is displayed in Figs. 2(a) and 2(b).

evant charge states in which both the initial and final configurations are local minima of the potential energy surface. The charge state is kept fixed during the search. However, the thermodynamically preferred charge state at the final site may differ from that at the initial site for a given value of  $\mu_F$ . In this situation we assume that the migration takes place in the initial charge state and the defect charge state adjusts only at the final site to the more favorable value. Regarding the migration of boron-vacancy complexes  $B_C-V_C$  we adopted the drag-method outlined in Ref. 27.

### III. MIGRATION OF THE INTERSTITIAL

#### A. Interstitial configurations in 3C-SiC

Before turning to the details of the interstitial-mediated boron migration it is important to identify the stable and metastable interstitial sites. The nature of the stable sites determines whether the migration takes place via a kick-out/kick-in mechanism or via an interstitialcy mechanism. The fact that boron interstitials are typically charged gives rise to a multitude of such sites with strong Fermi-level dependent energetics. The Fermi-level effect is hence an important factor in the boron migration. In Fig. 1 we have plotted the formation energy of the most important interstitial configurations in 3C-SiC. Table I lists the corresponding ionization levels. Three distinct ground state configurations are identified: the carbon-coordinated tetrahedral site  $B_{TC}$  ( $p$ -type), the hexagonal site  $B_{Hex}$ , and a split-interstitial  $B_{spSi\langle 110 \rangle}$  at the silicon site ( $n$ -type) which consists of an essentially  $\langle 110 \rangle$ -oriented boron-silicon dumbbell [cf. Fig. 2(a)].

Note that in Fig. 1  $B_{TC}$  only appears in the charge state  $3^+$ . It possesses an unoccupied localized state slightly above the artificially low Kohn-Sham conduction band edge. Due to the similarity of  $B_{TC}$  with the corresponding silicon interstitial  $Si_{TC}$  we adopted the approach of Ref. 27 and plotted the

TABLE I. Ionization levels of interstitial boron and boron complexes with interstitials and vacancies in 3C-SiC.

	$(2^+ 3^+)$	$(1^+ 2^+)$	$(0 1^+)$	$(1^- 0)$
Interstitials				
$B_{TC}$	$\sim 1.1$			
$B_{Hex}$	0.3	0.8	1.9	
$B_{spSi\langle 110 \rangle}$		0.3	1.0	1.5
$B_{spSi\langle 100 \rangle}$			1.5	2.0
$B_{spC\langle 100 \rangle}$			1.5	1.9
$B_{spC\langle 110 \rangle}$			1.6	2.0
$B_{bc}$			1.6	2.2
Complexes with interstitials				
$B_{Si-Si_{sp\langle 110 \rangle}}$			0.7	1.4
$B_C-C_{sp\langle 100 \rangle}$			1.2	1.9
$B_C-C_{spSi\langle 100 \rangle}$			1.3	1.8
$B_{Si-C_{sp\langle 100 \rangle}}$				
$(BC)_{Si}$			1.2	1.7
$(BC)_{Hex}$			1.9	1.4
$(B_2)_{Si}$			0.5	2.1
Complexes with vacancies				
$B_{Si-V_C}$			1.8	2.1
$B_C-V_C$			1.6	1.4

formation energy of  $B_{TC}^{3+}$  up to the value of  $\mu_F$  where this level would get occupied.  $B_{Hex}$  is unstable in the charge state  $3^+$  and relaxes into the  $B_{TC}$ -site. The formation energy of  $B_{Hex}^{2+}$  is plotted in Fig. 1 to the value of  $\mu_F$  where the charge state  $3^+$  becomes relevant.

In addition to these sites, there are other metastable sites, that serve as intermediate sites for the interstitial migration. The tetrahedrally silicon coordinated site  $B_{TSi}$  has a much higher formation energy than the  $\langle 100 \rangle$ -oriented split interstitials  $B_{spSi\langle 100 \rangle}$ ,  $B_{spC\langle 100 \rangle}$  on the silicon and carbon sublattice [cf. Fig. 2(b)]. A split interstitial at the carbon site ( $B_{spC\langle 110 \rangle}$ ) and the bond-centered site  $B_{bc}$ , which may be interpreted as a  $\langle 111 \rangle$ -oriented split interstitial at a carbon site (not included in Fig. 1) are slightly less stable than the  $\langle 100 \rangle$ -oriented interstitials.

Our finding of a higher stability of the hexagonal interstitial in comparison with the split interstitial sites for  $\mu_F < 1.9$  eV is in good agreement with the recent analysis of Rurali *et al.*<sup>19</sup> for the neutral interstitials.

#### B. Interstitial configurations in 4H-SiC

In 4H-SiC additional sites are available for the interstitial atoms. These sites originate from the alternating cubic and hexagonal stacking sequence of this polytype (cf. Fig. 3). The cubic lattice planes enclose the tetrahedrally carbon or silicon coordinated sites as described for 3C-SiC above. The hexagonal planes resemble the wurtzite structure of 2H-SiC. The interstice of the wurtzite lattice is characterized by a tetrahedral site surrounded by four carbon and four silicon

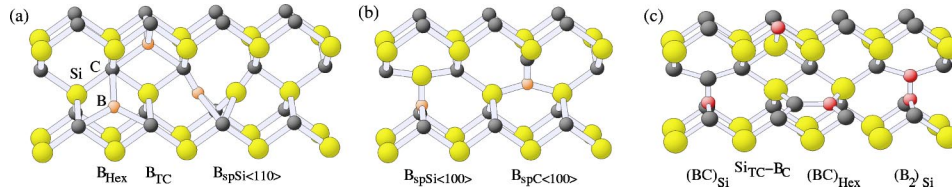


FIG. 2. Boron interstitials in 3C-SiC: geometry of (a) the most stable boron interstitials, (b) the intermediate sites  $B_{spSi(100)}$  and  $B_{spC(100)}$ , and (c) the boron complexes  $(BC)_{Si}$ ,  $Si_{TC}-B_C$ ,  $(BC)_{Si}$ , and  $(B_2)_{Si}$ .

atoms and an open cage encompassed by two hexagonal rings of the lower and upper basal plane. Thus, due to the stacking sequence, hexagonal sites located close to the (cubic or hexagonal) basal plane are distinct from those located in the perpendicular lattice planes. The boron split-interstitials are always located at the boundary between a cubic and a hexagonal plane. Hence the orientation of the B-C or B-Si dumbbell of the  $\langle 100 \rangle$  and  $\langle 110 \rangle$  split-interstitials is important. The dopant atom either lies in a cubic or a hexagonal plane, resulting in structural and energetic differences between these two types. Since the resulting complex picture of the formation energies and ionization levels in 4H-SiC does not add much essential information to Fig. 1, we only briefly summarize the differences below.

The formation energies of the defects at cubic sites differ only within 0.5 eV from their counterparts in 3C-SiC. As in 3C-SiC the tetrahedrally carbon coordinated interstitial  $B_{TC,k}$  is the energetically most favorable interstitial in  $p^+$ -type material. At  $\mu_F > 0.6$  eV the hexagonal interstitial located in the basal plane  $B_{Hex,b-h}$  is preferred over  $B_{TC,k}$ . The interstitial located in the perpendicular hexagonal rings  $B_{Hex,k}$  and  $B_{Hex,h}$  are slightly higher than  $B_{Hex,b-h}$ . As in 3C-SiC the hexagonal interstitial is essentially threefold carbon coordinated. This type of bonding is energetically more favorable for  $B_{Hex,b-h}$  within the 2H-like hexagonal basal-plane. The tetrahedral site with carbon and silicon neighbors ( $B_{TCsi}$ ) is found to be unstable. The boron atom relaxes into the  $B_{Hex,b-h}$  site. The ionization levels of the hexagonal interstitials essentially correspond to the findings for  $B_{Hex}$  in 3C-SiC (within 0.3 eV).

As in 3C-SiC, the split interstitial configurations are preferred for  $n$ -type material. For  $\mu_F$  above 1.9 eV  $B_{spC(100)}$  and

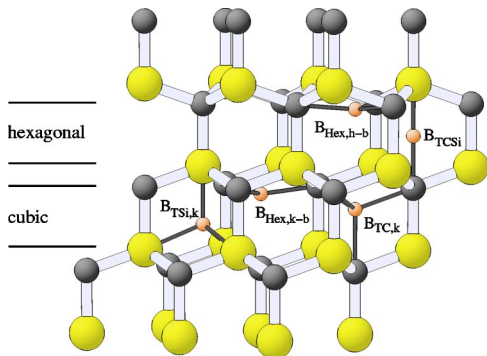
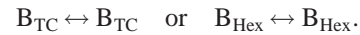


FIG. 3. Interstitials in 4H-SiC: geometry of the hexagonal and cubic interstice. The interstitial sites  $B_{TC,k}$ ,  $B_{TSi,k}$  and  $B_{Hex,b-k}$  in the cubic interstice, and  $B_{Hex,h-b}$  and (unstable)  $B_{TCsi}$  in the hexagonal interstice are indicated.

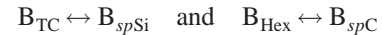
$B_{spSi(110)}$  are the most favorable boron interstitials. As mentioned above, the orientation of the split interstitial is important: in both cases the location of the boron interstitial within the cubic plane is preferred. The energetic difference between the split-interstitials with different orientations can amount to 0.5 eV. At the hexagonal site  $B_{spSi(110)}$  is unstable with B oriented toward the hexagonal interstice. Due to the minor differences between the defect hierarchy in 3C and 4H-SiC we expect that our results for the boron migration in 3C are transferable to 4H-SiC, and also to 6H-SiC. In the latter polytype the stacking sequence is two cubic planes followed by a hexagonal plane. Hence the same defects as discussed for 4H-SiC should also be present in 6H-SiC.

### C. Migration mechanisms

The migration of the boron interstitial takes place between the stable sites either directly or via a breakpoint at an intermediate metastable site. In Table II we list the energy barriers for the migration between the most relevant sites. The tetrahedral and hexagonal interstitials may migrate through the open interstice. The migration paths are



The migration may also proceed via the split-interstitial configurations



as intermediate sites ( $B_{spSi}$  and  $B_{spC}$  refer to the  $\langle 100 \rangle$ -orientation regarding the positive and neutral interstitials). The direct migration path of  $B_{TC}$  avoids the  $B_{TSi}$ -site. The saddle point, however, is located near this site. In case of the direct migration of  $B_{Hex}$ , one has to distinguish between adjacent hexagonal sites either having one or two common carbon neighbors. The saddle point with a large barrier separates the former sites and is located near the  $B_{TSi}$ -site. The latter are connected via a smaller barrier of  $\sim 0.2$  eV.<sup>7</sup> The direct migration path of  $B_{Hex}$  inevitably includes both situations and thus the larger barrier determines the migration barrier of  $B_{Hex}$ .

A comparison of the migration barriers shows that the route via the split-interstitial sites is preferred. Even though  $B_{spSi(110)}^{2+}$  is more favorable than  $B_{spSi(110)}^{3+}$  the charge state may not change at the intermediate site, due to the small barrier of 0.1 eV. The boron interstitial most likely immediately continues to an adjacent  $B_{TC}$ -site, before such a conversion happens.

The migration of  $B_{Hex}^+$  and  $B_{Hex}^0$  may proceed via the energetically more favorable  $\langle 100 \rangle$ -oriented split-interstitials.

TABLE II. Boron migration: interstitial migration and kick-out/kick-in barriers in comparison to vacancy-mediated migration mechanisms in 3C-SiC. The shorthand  $B_{spC}$  refers to  $B_{spC(100)}$ .  $B_{spSi}$  implies  $B_{spSi(110)}$ , except for the charge states  $1^+$  and  $0$  where we refer to  $B_{spSi(100)}$ .

	Energy barrier [eV]									
	3+		2+		1+		0		1-	
	→	←	→	←	→	←	→	←	→	←
Interstitial										
$B_{TC} \leftrightarrow B_{TC}$	3.5									
$B_{Hex} \leftrightarrow B_{Hex}$			2.2		1.6		0.7			
$B_{TC} \leftrightarrow B_{spSi}$	3.0	0.1								
$B_{Hex} \leftrightarrow B_{spSi}$			2.0	0.1	1.2	0.2	0.6	0.1		
$B_{Hex} \leftrightarrow B_{spC}$					1.3	0.3	0.8	0.2		
$B_{spSi} \leftrightarrow B_{spSi}$					0.4		0.5		1.1	
$B_{spSi} \leftrightarrow B_{spC}$					0.5	0.5	0.3	0.1	0.9	0.4
Kick-out/kick-in										
$Si_{TC}-B_{Si} \rightarrow B_{TC}$	1.1	4.6								
$Si_{sp}-B_{Si} \leftrightarrow B_{spSi}$					0.3	4.0	0.8	3.9	1.3	3.8
$C_{sp}-B_C \leftrightarrow B_{spC}$					0.6	2.0	0.1	1.0	0.1	0.6
$C_{spSi}-B_C \rightarrow B_{Hex}$			1.1	3.2	1.5	2.9	0.8	1.5		
$C_{spSi}-B_C \rightarrow B_{spSi}$									2.1	2.6
$B_{Si}+C_{sp} \rightarrow (BC)_{Si}$					0.7	3.8	0.6	3.6	0.7	3.0
$(BC)_{Si} \rightarrow B_{Hex}-C_{Si}$					5.7	1.3	5.7	0.8		
$(BC)_{Si} \rightarrow B_{spSi}-C_{Si}$									5.3	0.7
$B_C-Si_{TC} \rightarrow B_{TC}-Si_C$	4.1	1.5								
$B_C-Si_{TC} \rightarrow Si_{TC}+B_C$	3.7	2.2								
Vacancy										
$B_{Si}-V_C \leftrightarrow B_C-V_{Si}$							4.5	0.1	3.7	0.5
$B_{Si}-V_{C_{c.e.1}} \leftrightarrow B_C-V_{Si}$					9.4			8.0		6.4
$B_{Si}-V_{C_{c.e.2}} \leftrightarrow V_C-B_{Si}$					9.5			9.2		7.2
$B_{Si}-V_C \leftrightarrow V_C-B_{Si}$					4.9			4.3		3.6
$B_C-V_C \leftrightarrow V_C-B_C$					3.6			3.0		2.3
$B_C-V_{C_1} \leftrightarrow V_C-B_C$					4.2			4.6		4.1
$B_C-V_{C_2} \leftrightarrow V_C-B_C$					5.7			5.3		5.3

Also in this case, we find that the intermediate split interstitial sites are not very stable. Along the path, boron shifts essentially sideways toward its silicon or carbon neighbors in the hexagonal ring, thus breaking a minimal number of bonds with its carbon neighbors. Also a migration via  $\langle 110 \rangle$ -oriented split-interstitials and  $B_{bc}$ -site is possible. The path between these sites and  $B_{Hex}$  will involve the  $B_{spC(100)}$ -site or its neighborhood. Since  $B_{spC(110)}$  and  $B_{bc}$  are energetically equivalent to the  $\langle 100 \rangle$ -oriented site we expect similar or larger barriers. Regarding  $B_{Hex}$  our analysis is in agreement with the path investigated by Rurai *et al.*<sup>19</sup>

Turning to the migration between adjacent split-interstitial sites

$$B_{spSi} \leftrightarrow B_{spSi}, B_{spSi} \leftrightarrow B_{spC} \quad \text{and} \quad B_{spC} \leftrightarrow B_{spC}$$

by nearest or second nearest neighbor hops, we note that the positive and neutral split-interstitials are not very stable. With a low probability a boron split-interstitial may also migrate to a neighboring silicon or carbon site. Only for a Fermi-level above 1.9 eV the migration between adjacent split-interstitial sites becomes a dominant process.  $B_{spSi(110)}^-$  migrates via carbon sites ( $B_{spC(100)}$ ) and with a slightly higher barrier also by second neighbor hops on the silicon sublattice.  $B_{spSi(110)}^-$  may also switch its orientation. This process, that is connected with a barrier of 0.9 eV, enables an isotropic migration of the split-interstitial. The migration of

$B_{spSi\langle 110 \rangle}^-$  corresponds to the interstitialcy mechanism since the silicon-boron pair remains coupled.

The migration is governed by a barrier of 3.0 eV ( $B_{TC}$ ) for a Fermi level below 0.7 eV and a barrier of 0.9-1.2 eV ( $B_{Hex}^+$  and  $B_{spSi\langle 110 \rangle}^-$ ) above this value. The smaller barrier of 0.6 eV ( $B_{Hex}^0$ ) takes effect only in the small window between 1.9 eV and 2.0 eV and should be hardly relevant.

#### IV. KICK-OUT/KICK-IN REACTIONS

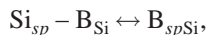
The boron diffusion by the kick-out or the interstitialcy mechanism is initiated by an interaction with self-interstitials. We first discuss the kick-out reactions of  $B_{Si}$  and  $B_C$  with the corresponding silicon or carbon interstitial, followed by the kick-out reactions with interstitials of the other species. At the end of this section we turn to the kick-in reactions and its preference for the carbon sublattice.

##### A. $B_{Si}$ and silicon interstitials

For the substitutional boron at the silicon site ( $B_{Si}$ ) we consider reactions with the tetrahedral carbon-coordinated silicon interstitial  $Si_{TC}$ , i.e.,



and the  $\langle 110 \rangle$ -oriented split-interstitial, i.e.,

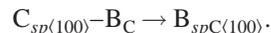


which are the dominant silicon interstitial configurations for  $\mu_F < 1.2$  eV and  $\mu_F > 1.2$  eV, respectively.<sup>27</sup> The reaction with  $Si_{TC}^{4+}$  occurs when the interstitial has reached an interstitial site next to the ionized boron acceptor  $B_{Si}^-$  and drives the boron into an adjacent  $B_{TC}$ -site. The kick-out barrier of 1.1 eV is much smaller than the migration barrier of  $Si_{TC}$  that amounts to 3.5 eV. The kick-out yields a considerable energy gain of 3.5 eV. The reaction with  $Si_{sp\langle 110 \rangle}$  starts with the formation of the complex  $B_{Si}-Si_{sp\langle 110 \rangle}$  that exists in positive or negative charge states (cf. Table I for the ionization levels). For the positive and neutral complex a boron split-interstitial is formed as an intermediate configuration at the silicon site before the boron-interstitial reaches an adjacent hexagonal site. The barriers for the reaction are given in Table II. They are smaller than or equal to the migration barrier of  $Si_{sp\langle 110 \rangle}$  that amounts to 1.4 eV. Again a considerable energy gain of 3.6–4.7 eV is associated with the complete kick-out process. This implies that rather large barriers are encountered for the kick-in reaction of  $B_{TC}$  and  $B_{Hex}$  as well as the dissociation of the  $B_{spSi\langle 110 \rangle}^-$  configurations into  $B_{Si}^-$  and  $Si_{sp\langle 110 \rangle}^0$ . The values range between 4.6 eV ( $B_{TC}$ ) and 3.8 eV ( $B_{spSi\langle 110 \rangle}^-$ ) and exceed the migration barriers of the boron and silicon interstitial.

##### B. $B_C$ and carbon interstitials

Regarding the substitutional boron on the carbon sublattice  $B_C$ , we analyzed reactions with the carbon split-interstitials  $C_{sp\langle 100 \rangle}$  and  $C_{spSi\langle 100 \rangle}$  at a neighboring carbon and silicon site, respectively. The interaction with silicon intersti-

entials is discussed below.  $C_{sp\langle 100 \rangle}$  and  $C_{spSi\langle 100 \rangle}$  are the dominant carbon interstitials in SiC.<sup>27</sup> In both cases boron-carbon interstitial complexes form before the actual kick-out reaction takes place. The complexes exist in positive and negative charge states (cf. Table I). We consider the reaction



Since  $B_{spC\langle 100 \rangle}$  is not very stable, the boron interstitial will proceed with a high probability to a more favorable interstitial site. An inspection of Table II shows that the barriers for this whole kick-out reaction are fairly small, in particular for the neutral and negative boron carbon-interstitial complex. In fact, they are even smaller than the migration barrier of  $C_{sp\langle 100 \rangle}$ . At typical diffusion temperatures the arrival of  $C_{sp\langle 100 \rangle}$  at a carbon site neighboring  $B_C$  should suffice to trigger the kick-out reaction.

For  $C_{spSi\langle 100 \rangle}$  we consider a kick-out directly to the next  $B_{Hex}$  or  $B_{sp\langle 110 \rangle}$  site for the positive/neutral and negative charge state, respectively, i.e.,

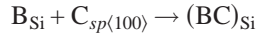


The barriers for this reaction are larger than those for the  $B_C-C_{sp\langle 100 \rangle}$  complex which is formed before the carbon interstitial reaches the silicon site next to  $B_C$ . Therefore this reaction may not be important for the kick-out process, but it still facilitates a pathway for the kick-in reaction. In both cases an energy gain is associated with the kick-out reaction that varies between 1.4 eV for the negative charge state and 2.4 eV for the positive charge state. The barriers for the kick-in reactions of  $B_{Hex}$  and the dissociation of  $B_{sp\langle 110 \rangle}$  are consequently high. The effective barrier for a kick-in of  $B_{Hex}$  via  $B_C-C_{sp\langle 100 \rangle}$  amounts to 3.0 eV for  $B_{Hex}^+$  and 1.8 eV for  $B_{Hex}^0$ , whereas 1.5 eV are obtained for the dissociation of  $B_{spSi\langle 110 \rangle}^-$ . These effective barriers are slightly higher than the barriers for a kick-in via  $B_C-C_{spSi\langle 100 \rangle}$  which thus has a higher probability. As before, these barriers exceed the migration barriers of the boron interstitial.

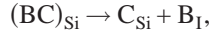
##### C. $B_{Si}$ and carbon interstitials

The kick-out reaction of  $B_{Si}$  with carbon interstitials eventually results in the formation of carbon antisites  $C_{Si}$ . Vice versa, the interaction of boron interstitials with antisites may annihilate  $Si_C$  or  $C_{Si}$ . The central point of our analysis is that stable boron-antisite complexes are formed in this process.

In the case of  $B_{Si}$  and  $C_{sp\langle 100 \rangle}$  the most stable complex results when the boron atom shares its site with the carbon atom forming a  $\langle 100 \rangle$ -oriented dumbbell at the silicon site  $(BC)_{Si}$  as shown in Fig. 1(c). The electronic structure of  $(BC)_{Si}$  was already described by Aradi *et al.*<sup>32</sup> in their analysis of possible candidates for the deep boron acceptor. Our results for the ionization levels are given in Table I. The interaction of a carbon split interstitial and  $B_{Si}$  via the reaction



yields an energy gain between 3.3 and 3.7 eV, depending on its charge state. Its dissociation into a boron-interstitial and a carbon antisite via



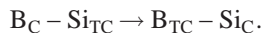
where  $B_I$  stands for  $B_{Hex}^{+/0}$  or  $B_{spSi}^-$ , costs between 4.1 and 5 eV [ $(CB)_{Si}^+$  and  $(CB)_{Si}^-$ ] with respect to the isolated defects. It is interesting to note that the  $B_{Hex}$ -site with a neighboring antisite is unstable and transforms into the more stable  $(BC)_{Si}$ -complex. Thus the antisite captures any boron interstitial that arrives at this hexagonal site.

We have also calculated the reaction barriers for these processes. For the reaction  $B_{Si} + C_{sp(100)} \rightarrow (BC)_{Si}$  we started with the interstitial located at the fourth neighbor carbon site, since the nearest neighbor complex  $C_{sp(100)}-B_{Si}$  transformed into a bond-centered configuration, which was only 1.0 eV less favorable than  $(BC)_{Si}$ . In the above reaction the interstitial carbon atom hops to the carbon neighbor of  $B_{Si}$ . It displaces this atom towards the boron site such that a  $(BC)_{Si}$ -complex is formed. The hopping carbon interstitial becomes the neighbor of this complex. The barriers for the formation of the complex are comparable to the migration barrier of the split interstitial (cf. Table II). Regarding the capture of  $B_{Hex}$  by  $C_{Si}$  we considered a hexagonal site located in the  $\langle 111 \rangle$ -direction. The barrier for the capture of  $B_{spSi}^-$  was calculated starting with  $B_{spSi}$  as a second neighbor of  $C_{Si}$ . The resulting barriers vary between 1.3 eV ( $B_{Hex}^+$ ) and 0.7 eV ( $B_{spSi}^-$ ) and are comparable to the migration barrier of the hexagonal interstitial (cf. Table II). Obviously, the dissociation of  $(BC)_{Si}$  into a  $B_{Si}$  and  $C_{sp(100)}$  has lower barriers than the ejection of a boron-interstitial (the values differ by 1.7 eV). This means that carbon antisites are annihilated through this process and the boron interstitial is converted into a shallow acceptor.

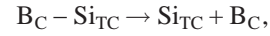
#### D. $B_C$ and silicon interstitials

The interaction of  $B_C$  with a silicon interstitial leads either to a complex with  $Si_{TC}$  or  $Si_{sp(110)}$ . A complex  $(BSi)_C$  was found to be unstable. The complex  $B_C-Si_{TC}$  forms with an energy gain of 3.6 eV from the isolated defects  $B_C$  and  $Si_{TC}$ . In 3C-SiC the complex has no defect states within the band gap and exists only in the charge state  $3^+$ . Complexes with  $Si_{sp(110)}$  are by far less stable than  $B_C-Si_{TC}$  and have a dissociation energy of 1.8 eV or below depending on the charge state. Most likely  $B_C-Si_{sp(110)}$  transforms into  $B_C-Si_{TC}$ . We therefore concentrate on this latter complex.

The kick-out reaction converts  $B_C-Si_{TC}$  into a silicon antisite and a boron interstitial



The dissociation energy of  $B_{TC}-Si_C$  is only 0.6 eV with respect to the isolated boron interstitial  $B_{TC}$  and antisite  $Si_C$ . The kick-out barrier amounts to 4.1 eV. For the ejection of  $Si_{TC}$  from  $B_C-Si_{TC}$  into a neighboring  $Si_{TC}$ -site, i.e.,



we obtain a barrier of 3.7 eV, which is comparable to the former barrier. The energy difference between the sites amounts to 1.5 eV and is lower than the energy for the dissociation into isolated defects of 3.6 eV. This means that a long range interaction between  $Si_{TC}$  and  $B_C$  exists. Taking this and the migration barrier of  $Si_{TC}$  (3.5 eV) into account, we may conclude that the dissociation of  $Si_{TC}-B_C$  into a  $Si_{TC}$  and  $B_C$  is associated with similar or higher activation energy than the kick-out reaction of the boron interstitial.

An important result is that the kick-out of  $B_{Si}$  by carbon interstitials is kinetically hindered. Furthermore, carbon antisites can enhance the incorporation of boron into the silicon sublattice. Instead, the kick-out of  $B_C$  has a much higher probability than the kick-out of  $B_{Si}$  by .

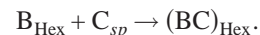
#### E. Site preference of the kick-in process

A key question is whether  $B_{Si}$  or  $B_C$  is preferentially formed by the kick-in/dissociation process. A comparison shows that the reactions that generate the shallow acceptor  $B_{Si}$  have by 1–2 eV higher barriers than those leading to  $B_C$ . Only for a Fermi-level position below 0.7 eV the kick-in into the silicon site should be favored. In this case  $B_{TC}^{3+}$  dominates and the complex  $B_{spC(100)}$  is unstable in this charge state. The only route that could result in  $B_C$  involves  $B_{Hex}^{2+}$  and requires charge transfer processes. For a Fermi level above 0.7 eV kinetic processes favor the formation of  $B_C$  over  $B_{Si}$ .

#### V. STABLE CLUSTERS WITH BORON INTERSTITIALS

The formation of thermally stable complexes of boron with other defects like self-interstitials potentially retards the boron diffusion. This may occur, for example, in the course of the annealing of implanted boron profiles. During the boron implantation carbon or silicon interstitials are generated in excess and may readily form clusters with boron atoms. The relevance of such a boron recapture has recently been discussed for carbon interstitials.<sup>33</sup> It was found that microscopic clusters comprised of two carbon atoms like the di-carbon antisite and the hexagonal carbon di-interstitials have a large dissociation energy in the range of 4–5.6 eV.<sup>33–36</sup> Examples of stable boron complexes are  $(BC)_{Si}$  and  $B_C-Si_{TC}$ , which we discussed in the previous section. Now we consider complexes with boron interstitials in 3C-SiC as depicted in Fig. 2(c).

A very stable defect is the hexagonal boron-carbon interstitial  $(BC)_{Hex}$  [cf. Fig. 2(c)]. The boron-carbon interstitial pair binds to their neighbors in the hexagonal ring, breaking the corresponding silicon-carbon bonds of the ring. This is enabled by the  $sp^2$ -like hybridization of the interstitial pair. A localized defect state arises within the band gap from the unpaired  $p$ -orbitals of the interstitial-pair.  $(BC)_{Hex}$  exists in the positive and negative charge states. The neutral charge state is metastable due to a negative- $U$  effect.  $(BC)_{Hex}$  is formed according to the reaction



The dissociation of  $(BC)_{Hex}$  is associated with an energy cost of 3.5 eV for  $(BC)_{Hex}^+$  and 4.3 eV for  $(BC)_{Hex}^-$ .

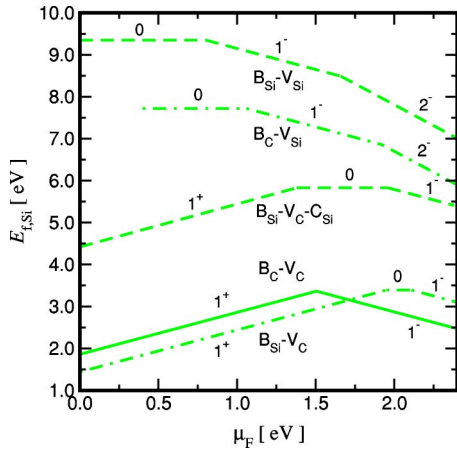


FIG. 4. Boron-vacancy complexes: formation energy for Si-rich conditions. The geometry of  $B_{Si}-V_C$  and  $B_C-V_C$  is displayed in Figs. 5(a) and 5(d).

Among the complexes of a boron interstitial with silicon interstitials we did not find particularly stable configurations. The most stable one is a pair of  $B_{Hex}$  and  $Si_{TC}$ . It has a dissociation energy of 1 eV or below, depending on the charge state. A hexagonal boron-silicon interstitial is unfavorable due to the rather extended silicon orbitals.

Regarding diboron clusters we first discuss complexes of a boron interstitial with  $B_{Si}$  or  $B_C$ . In both cases a boron-pair forms at the substitutional site which is oriented in the  $\langle 100 \rangle$ -direction. The electronic structure resembles that of the dicarbon antisite.<sup>37</sup> The complex at the silicon site  $(B_2)_{Si}$  is essentially neutral with ionization levels close to the band edges (cf. Table I). Its dissociation is associated with an energy cost of 3.1 eV. The corresponding complex  $(B_2)_C$  at the carbon site exists only in the positive and neutral charge state. Its ionization level is located close to the valence band edge.  $(B_2)_C$  has an almost vanishing dissociation energy and hence is not relevant.

Regarding complexes of two boron-interstitials we have investigated different configurations of a hexagonal diboron interstitial  $(B_2)$  and a complex of neighboring split-interstitials  $B_{spSi}-B_{spC}$ . The latter is the most stable complex. It has a dissociation energy of 1.7–2.4 eV, depending on its charge state (cf. Table I).

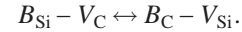
The above analysis indicates that stable boron complexes that may lead to a retardation of the boron diffusion do exist.

The boron complexes with intrinsic interstitials  $(CB)_{Si}$ ,  $B_C-Si_{TC}$ , and  $(CB)_{Hex}$ , and the diboron complex  $(B_2)_{Si}$  have substantial binding energies. This list, however, is incomplete and other stable boron complexes may exist.

## VI. VACANCY-RELATED MECHANISMS

### A. Stable boron-vacancy complexes

Boron-vacancy complexes are the diffusion vehicle for the vacancy-mediated boron-diffusion. Mobile nearest or second nearest neighbor complexes are formed when a vacancy migrates to a substitutional boron acceptor  $B_{Si}$  or  $B_C$ . The complexes  $B_{Si}-V_C$  and  $B_C-V_{Si}$  are comprised of a substitutional boron with a vacancy as a nearest neighbor. In the complexes  $B_C-V_C$  and  $B_{Si}-V_{Si}$  the boron atom and the vacancy are second neighbors. Figure 4 shows their formation energy for Si-rich conditions. In Figs. 5(a) and 5(d) the geometry of the most stable complexes  $B_{Si}-V_C$  and  $B_C-V_C$  is depicted. The nearest neighbor complexes  $B_{Si}-V_C$  and  $B_C-V_{Si}$  transform into each other with the boron atom switching between the carbon and silicon site



$B_{Si}-V_C$  was reported to be the most stable configuration already in earlier calculations.<sup>7,17,32,38</sup> It exists as a positive, neutral, and negative complex.  $B_C-V_{Si}$  is unstable in the positive charge state and exists as a neutral or negative complex. The positive charge state is therefore not shown in Fig. 4. Also the neutral complex transforms with a small barrier into  $B_{Si}-V_C$  (cf. Table II). The transformation of the negative complexes involves somewhat larger barriers of 0.5 and 1.1 eV for  $(B_C-V_{Si})^-$  and  $(B_C-V_{Si})^{2-}$ , respectively.

The second neighbor complex  $B_C-V_C$  is stable in the positive and negative charge state. Similar to the isolated carbon vacancy,<sup>27,39,40</sup> it exhibits a negative- $U$  behavior. The complex  $B_{Si}-V_{Si}$  is metastable in all charge states. With a displacement of the common carbon neighbor of  $B_{Si}$  and  $V_{Si}$  into the vacancy it transforms into the more stable  $B_{Si}-V_C-C_{Si}$ -complex with an energy gain between 4.9 and 2.3 eV. Its metastability has a similar origin as that of the silicon vacancy that transforms into  $V_C-C_{Si}$  for a Fermi-level position below 1.7 eV.<sup>17,27,41</sup>

### B. Migration of $B_{Si}-V_C$

For the migration of  $B_{Si}$  we have analyzed mechanisms based on the migration of  $B_{Si}-V_C$ . The complex  $B_{Si}-V_C$  could

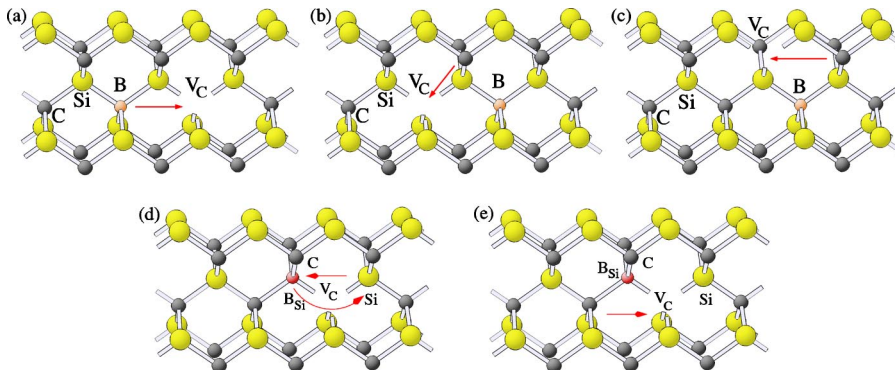


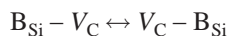
FIG. 5. Migration of the boron-vacancy complexes. Upper panel:  $B_C-V_C$ : (a) initial hop of the boron atom, (b) hop of carbon neighbor  $C_1$ , and (c) hop of carbon neighbor  $C_2$ . Lower panel:  $B_{Si}-V_C$  (d) concerted exchange of  $B_{Si}$  and Si and (e) site change of  $V_C$  by a second neighbor hop of a C-neighbor.

migrate by a ring mechanism<sup>42,43</sup> based on nearest neighbor hops



However, as shown in our earlier analysis,<sup>7</sup> this mechanism is not very likely. This is especially true for the positively charged complex, since the first exchange of boron and the vacancy leads to the unstable complex  $B_C - V_{Si}$ . Also the neutral complex  $B_C - V_{Si}$  is hardly stable, due to the small barrier of 0.1 eV (cf. Table II). Only for the negative complex a stabilizing barrier is observed. Taking further into account that  $V_C$  and  $V_{Si}$  migrate by second neighbor hops, a ring mechanism based on nearest neighbor hops does not seem likely.

Instead, the migration of  $B_{Si} - V_C$  could proceed by a concerted exchange of the boron and a silicon neighbor of the vacancy,



as depicted in Fig. 5(d). A migration of  $V_C$  by the second neighbor hop, as indicated in Fig. 5(e), moves the whole complex into a new position. For the concerted exchange we have investigated the path of Fig. 5(d) (denoted *c.e.1*) and a second path with the routes of B and Si exchanged (denoted *c.e.2*). The migration barriers are listed in Table II. Both exchange processes are associated with large barriers, those for path *c.e.1* being somewhat lower. The energy barriers of the second neighbor hop of the vacancy are much lower than the values obtained for the concerted exchange. Given the high migration barrier, the complex may also dissociate. The dissociation barrier can be estimated from the migration barrier of the carbon vacancy (5.2 eV for  $V_C^{2+}$ , 4.2 eV for  $V_C^+$ , and 3.5 eV  $V_C^0$  as obtained in Ref. 27) and the binding energy of the complex, which amounts to 2.3, 1.7, and 0.7 eV for the positive, neutral, and negative complex, respectively. By this approximation we obtain values between 7.5 and 4.2 eV. Thus the dissociation of  $B_{Si} - V_C$  is indeed more likely than the migration.

### C. Migration of $B_C - V_C$

For the migration of  $B_C$  via  $B_C - V_C$  we have analyzed a mechanism based on second neighbor hops



as depicted in Fig. 5. Three distinct hops are possible: a hop of  $B_C$  into  $V_C$  and hops of two different carbon neighbors that are common to  $V_C$  and  $B_C$ . These latter hops change the position of the vacancy with respect to  $B_C$ . The barriers for the three hops are listed in Table II. The lowest barrier is associated with the hop of  $B_C$ . The barriers for the hops of the carbon atoms are equal to or exceed the migration barrier of the isolated vacancy. The complex may also dissociate ( $B_C - V_C \rightarrow B_C + V_C$ ) after the boron has switched site with the vacancy. The dissociation barrier estimated from the migration barrier of  $V_C$  and the binding energy of the complex amounts to 6.5 and 4.2 eV for the positive and negative charge states, respectively. For the negative charge state the dissociation thus has a higher probability than the two carbon hops.

### D. Migration of $B_{Si} - V_C - C_{Si}$

The complex  $B_{Si} - V_C - C_{Si}$  should be mobile, as it is the case for  $V_C - C_{Si}$ .<sup>27</sup> A possible migration mechanism may involve a transformation into  $B_{Si} - V_{Si}$ . This configuration can migrate by second neighbor hops similar to  $B_C - V_C$ . The analysis of the full mechanism is complex, as a number of different intermediate configurations arise due to the metastability of the complex. Such a task requires large super cells and exceeds the available computational resources. Instead, we shall use the barrier of the second neighbor hop of  $V_{Si}$  as an estimate. This barrier varies between 2.7 and 3.2 eV.<sup>27</sup> We further assume that the transformation between  $B_{Si} - V_C - C_{Si}$  and  $B_{Si} - V_{Si}$  is thermally activated. The effective migration barrier is then given by the formation energy difference of the two complexes and the estimate for the migration barrier of  $B_{Si} - V_{Si}$ . Its estimated value varies between 4.8 eV ( $\mu_F = E_C$ ) and 8.2 eV ( $\mu_F = E_V$ ), where  $E_C$  and  $E_V$  are the conduction and valence band edge, respectively. Thus only in *n*-type material a reasonably low barrier occurs for this migration mechanism. There the silicon vacancy also becomes available as a stable defect.<sup>27</sup>

### E. Dissociative mechanism

The dissociative mechanism consists of a spontaneous creation of a boron interstitial vacancy pair and the subsequent migration of the boron interstitial. By a recombination with another vacancy, the boron interstitial becomes substitutional again. The major contribution to the activation energy is given by the energy difference between the substitutional defect and the boron interstitial vacancy pair. In the case of  $B_{Si}$  the dissociation creates  $B_{Hex} - V_{Si}$  or  $B_{spSi} - V_{Si}$  pairs. However, all pairs with the interstitial in the fourth neighbor shell of the vacancy recombine without barrier. We therefore use the isolated defects for an estimate of the energy difference. It amounts to 10.2 eV for the reaction  $B_{Si}^0 \rightarrow B_{Hex}^+ + V_{Si}^-$  (11.6 eV, if we refer to  $B_{Si}^-$  and  $\mu_F = 1.2$  eV). For  $B_C$  we obtain a lower bound for the activation energy of 7.6 eV using the second neighbor complex  $B_{spC} - V_C$  as a reference. Using the isolated defects  $B_{Hex}^+$  and  $V_C^0$  and  $\mu_F$  the energy difference amounts to 9.3 eV at  $\mu_F = 1.2$  eV.

## VII. DISCUSSION

In the following we discuss our results in the light of recent experiments. In particular, we identify the interstitial-mediated migration as the dominant diffusion mechanisms and point out the importance of the Fermi-level effect. Our view is supported by experimental results for the equilibrium diffusion with a spatially constant boron concentration<sup>23</sup> and investigations on the in-diffusion from the surface<sup>8,9,16</sup> as well as implanted boron-profiles.<sup>10,12,13</sup>

### A. Equilibrium diffusion

The equilibrium diffusion is described by the concentration of mobile boron defects and their diffusivities. It is assumed that substitutional boron can freely convert into mobile complexes and vice versa, implying a sufficiently high

TABLE III. Activation energy of the interstitial and vacancy-mediated boron diffusion.

Path	Explicit	Activation energy $Q_A$ [eV]		Range of $\mu_F$ [eV]
		Si-rich	C-rich	
$B_{TC}^{3+}$	$5.1 + 3\mu_F - \Delta\mu_B$	5.1–7.2		$E_V - 0.7$
$B_{Hex}^+$	$4.7 + \mu_F - \Delta\mu_B$	5.5–6.6		0.7–1.9
$B_{Hex}^0$	$6.0 - \Delta\mu_B$	6.0		1.9–2.0
$B_{spSi(110)}^-$	$8.3 - \mu_F - \Delta\mu_B$	5.9–6.3		$2.0 - E_C$
$(B_{Si^-}V_C)^+$	$10.6 + \mu_F - \Delta\mu_B$	10.6–12.5		$E_V - 1.9$
$(B_{Si^-}V_C)^0$	$11.1 - \Delta\mu_B$	11.1		1.9–2.1
$(B_{Si^-}V_C)^-$	$11.9 - \mu_F - \Delta\mu_B$	9.5–9.8		$2.1 - E_C$
$(B_C - V_C)^+$	$7.4 + \mu_F - 2\Delta\mu_{Si} - \Delta\mu_B$	7.4–8.9	8.6–10.1	$E_V - 1.5$
$(B_C - V_C)^-$	$10.5 - \mu_F - 2\Delta\mu_{Si} - \Delta\mu_B$	8.1–9.0	9.3–10.2	$1.5 - E_C$

temperature for the thermal activation of these reactions. The diffusion constant is a sum of the contributions of boron interstitials and boron-vacancy complexes determined by the defect concentration and diffusivity. The activation energy for each mechanism is given by<sup>1</sup>

$$Q_A = E_f + E_m,$$

where  $E_f$  is the formation energy of the defect and  $E_m$  its migration barrier.  $E_f$  is a function of  $\Delta\mu_B$  and  $\mu_F$ . In case of the boron-vacancy complex  $B_C - V_C$  it also depends on  $\Delta\mu_{Si}$  (stoichiometry). The explicit expressions for  $Q_A$  are listed in Table III. The last column shows the range of  $\mu_F$  in which the charge state of the migrating defect is stable. For a comparison of the mechanisms we also included the variation of  $Q_A$  due to  $\mu_F$ -variation in the stoichiometry range ( $\Delta\mu_{Si} = 0.0$  eV and  $\Delta\mu_{Si} = -0.62$  eV, respectively). Note that the dependence on  $\Delta\mu_B$  is the same for all diffusion channels, as stated in the second column. An inspection shows that the interstitial-mediated diffusion always dominates over the vacancy-mediated mechanisms. Only in C-rich material with  $\mu_F > 2.0$  eV the migration of  $(B_C - V_C)^-$  and  $B_{spSi(110)}^-$  have a similar activation energy. This, however, is only relevant when the concentration of  $n$ -type dopants by far exceeds the

boron concentration, as we shall see below. Also with respect to the dissociative mechanism, the interstitial-mediated channel dominates.

For a comparison with diffusion experiments it is helpful to obtain a relation between  $\Delta\mu_B$  and the total boron concentration. Such a relation depends on the temperature and on the doping conditions via  $\mu_F$  which is obtained from the neutrality equation for a given value  $\Delta\mu_B$  as outlined in Sec. I. This relation is shown in Fig. 6 for 3C-SiC with a negligible content of other impurities. In Fig. 7 the Fermi level  $\mu_F$  is plotted versus the boron concentration for 3C-SiC and 4H-SiC.

As discussed in Sec. III, the Fermi-level position is important for the mechanism of the interstitial-mediated boron migration. At low boron concentrations the Fermi level is located at the mid-gap for the corresponding temperature. It is lower than the value at zero temperature ( $E_{gap}^{3C} = 2.39$  eV and  $E_{gap}^{4H} = 3.29$  eV) since the fundamental band gap shrinks at high diffusion temperatures. It decreases from its mid-gap

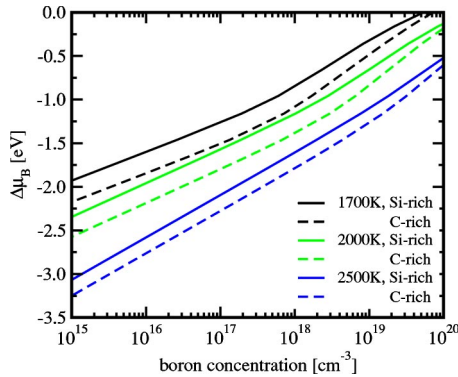


FIG. 6. Chemical potential  $\Delta\mu_B$  versus boron concentration for Si-rich and C-rich conditions for 3C-SiC.

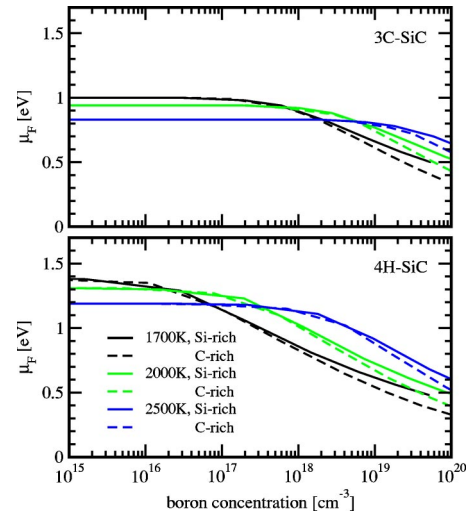


FIG. 7. Fermi-level  $\mu_F$  versus boron concentration for Si- and C-rich conditions. The upper panel refers to 3C-SiC, the lower panel to 4H-SiC.

value with increasing boron concentrations. At high concentrations (above  $10^{19} \text{ cm}^{-3}$ ) it approaches the acceptor levels of  $B_{\text{Si}}$  or  $B_{\text{C}}$  (the calculated values<sup>7</sup> amount to 0.2 and 0.4 eV, respectively; using the experimental value for  $B_{\text{Si}}$  (Ref. 44) of 365 meV does not affect the results). Note that  $B_{\text{Si}}$  was found to dominate in C-rich material, while  $B_{\text{C}}$  is relevant for Si-rich conditions.<sup>6,7</sup> Figure 7 shows that  $\mu_{\text{F}}$  may reach values below 0.7 eV for boron concentrations above  $5 \times 10^{18} \text{ cm}^{-3}$ . The interstitial-mediated boron diffusion thus is dominated by the hexagonal boron-interstitial  $B_{\text{Hex}}^+$  at low and moderate boron concentrations and by the tetrahedral carbon-coordinated boron interstitial at high boron concentrations. Note, however, that this concentration depends on the polytype and on the diffusion temperature.

Experimentally the equilibrium boron diffusion has been investigated by Mokhov and coworkers by means of tracer diffusion experiments in 6H-SiC in a temperature range of 2380–2860 K.<sup>23</sup> The analysis of the diffusion data yields an activation energy of 5.5 eV. The samples were boron-doped with a concentration of  $5 \times 10^{19} \text{ cm}^{-3}$ . This boron concentration at 2500 K corresponds to a value of  $\Delta\mu_{\text{B}}$  between  $-0.7$  eV (C-rich) and  $-0.6$  eV (Si-rich) and a Fermi level at 0.7 eV (Si-rich) and 0.6 eV (C-rich) for 6H-SiC. Under these conditions the diffusion proceeds via  $B_{\text{Hex}}^+$  with an activation energy of 6.0 eV (C-rich and Si-rich) which is in nice agreement with the experimental value.

### B. Evidence for the Fermi-level effect and the kick-out mechanism

The earlier in-diffusion experiments conducted by Mokhov *et al.*<sup>9</sup> in 6H-SiC evidenced that, indeed, a positively charged defect mediates the boron migration in *p*-type and intrinsic material. Though Mokhov *et al.* proposed a model based on boron-vacancy complexes, their analysis is in fact also valid for an interstitial mediated diffusion as suggested by our theoretical results and the detailed analysis of the diffusion profiles by Konstantinov.<sup>11</sup> Mokhov *et al.* used aluminum-doped samples with an Al concentration between  $2 \times 10^{17}$ – $10^{21} \text{ cm}^{-3}$  to analyze the Fermi-level effect of the boron in-diffusion. The diffusion coefficient extracted from the error-function shaped boron profiles in the temperature range 1600–2550 °C and for a moderate boron surface concentration  $\sim 10^{18} \text{ cm}^{-3}$  showed a linear dependence on the net acceptor concentration characteristic for a positively charged defect. Interestingly, for a temperature of 1950 °C the Fermi level effect was only observed for acceptor concentrations above  $10^{18} \text{ cm}^{-3}$ , while the diffusion coefficient was essentially insensitive to the Al-concentration below this value. This finding is consistent with the calculated dependence of  $\mu_{\text{F}}$  on the boron concentration at high temperatures (cf. Fig. 7): At 2500 K in 4H-SiC the Fermi-level deviates from its mid-gap value only for boron concentrations above  $10^{18} \text{ cm}^{-3}$ . Note that at these high temperatures the lower value for the aluminum acceptor level ( $E_{\text{V}}+200$  meV) is almost negligible in this respect.

The analysis of diffusion experiments on implanted boron profiles gave also evidence for a kick-out mechanism.<sup>12</sup> The experiments were conducted in *p*-type and *n*-type materials

( $[\text{Al}] \sim 4 \times 10^{16} \text{ cm}^{-3}$  and  $[\text{N}] \sim 10^{17} \text{ cm}^{-3}$  respectively) using implanted box-shaped boron profiles with an average boron concentration of  $5 \times 10^{18} \text{ cm}^{-3}$ . It was possible to consistently describe the diffusion profiles by a diffusion model based on the kick-out mechanism, while a model based on a dissociative mechanism was not applicable.

### C. Transient enhanced diffusion and coimplantation

In the description of the boron in-diffusion from the surface and of the diffusion of implanted boron profiles one inevitably has to include the kinetics of the kick-out/kick-in reactions, the diffusion of self-interstitials, and the excess concentration of self-interstitials generated by the implantation or during the in-diffusion from the surface.<sup>1,11,12</sup> In this and the following sections we briefly discuss such kinetic effects.

An excess of carbon or silicon interstitials was exploited to control the boron diffusion in the subsequent annealing after implantation by Laube *et al.*<sup>10</sup> They found that the transient enhanced boron diffusion was suppressed by the coimplantation of carbon or by preannealing the samples at a lower temperature than the main annealing (900 °C compared to 1700 °C), whereas a silicon coimplantation further enhanced the diffusion. It was argued<sup>10</sup> that the preannealing could reduce the implantation damage via interstitial-vacancy recombination and increase the activation of the dopant atoms. The efficiency of this processing step at moderate temperatures in the initially compensated material can be easily explained theoretically<sup>33</sup> by the low barriers encountered for the self- and boron-interstitial migration and for the vacancy-interstitial recombination. In contrast to the preannealing, the silicon or carbon coimplantation besides the additional damage should enhance the interstitial concentration and, hence, the boron-diffusion. The retardation effect of the carbon coimplantation is not obvious from this simple argument and thus Laube *et al.* argued, in analogy to the case of silicon, that interstitial carbon may form thermally stable defects with boron.

Indeed Mattausch *et al.*,<sup>34,37</sup> Gali *et al.*,<sup>36</sup> and Bockstedte *et al.*<sup>33</sup> have shown theoretically that carbon interstitials in SiC can form highly stable carbon aggregates. This clustering process may diminish the surplus of highly mobile carbon interstitials already during the implantation.<sup>33</sup> Even though these clusters release the interstitials at high diffusion temperatures, they give rise to a retardation effect. Since boron and carbon were implanted at similar doses, the formation of the boron-carbon interstitial cluster  $(\text{BC})_{\text{Hex}}$  may add to a retardation effect. This is indicated by the relatively large dissociation energy of the hexagonal boron-carbon interstitial discussed in Sec. V, which, however, is less stable than the corresponding carbon di-interstitial. A similarly stable silicon-boron complex was not found except for  $\text{Si}_{\text{TC}}\text{-B}_{\text{C}}$ . However, as discussed above, this complex affects the boron-diffusion in a different way.

Another possibly stronger retardation arises from the following observation: An excess of carbon interstitials has a different effect on the kick-out diffusion than an excess of silicon interstitials. While silicon interstitials initiate kick-out

reaction for  $B_{Si}$  and  $B_C$ , carbon interstitials predominantly interact with  $B_C$ . The kick-out reaction with  $B_{Si}$  is kinetically suppressed. The excess carbon also implies an enhanced concentration of carbon antisites and consequently of  $B_{Si}$ . As shown in Sec. IV, carbon antisites kinetically enhance the concentration of  $B_{Si}$ . Hence the transient effect is already reduced by these aspects in the case of carbon coimplantation.

#### D. Preferential formation of $B_C$ in diffusion tails

In the discussion of the kick-out/kick-in reactions in Sec. III we pointed out that the kick-in reaction  $B_{Hex} \rightarrow B_{Si} + Si_I$  has a considerably higher barrier than the corresponding reaction  $B_{Hex} \rightarrow B_C + C_I$ . We argued that this should lead to a preferential formation of  $B_C$  as compared to  $B_{Si}$  when thermodynamic equilibrium is not fully established. In particular, this argument should apply to the extended diffusion tails of in-diffused or implanted boron-profiles. At equilibrium, however, the distribution of boron on the carbon and silicon sublattice depends on the stoichiometry of the sample as demonstrated by theoretical investigations<sup>6,7</sup> in agreement with experiments,<sup>3,44</sup> i.e., at C-rich conditions the shallow acceptor  $B_{Si}$  dominates over  $B_C$ . Since all processes are stationary in the case of the equilibrium diffusion, such a kinetic effect is absent there. Experimental evidence for the preferential formation of deep boron centers was reported for the boron in-diffusion<sup>16</sup> and the diffusion of implanted boron profiles.<sup>15</sup> Gao *et al.*<sup>16</sup> used a *n*-type substrate to create a *p-n* diode by the in-diffused boron. They observed a donor-acceptor pair recombination involving the deep boron acceptor that, according to the interpretation of the experiment, stemmed from the second zone where the *p-n* transition was located. A corresponding transition involving the shallow acceptor was absent. For boron-implanted *n*-type 6H-SiC Gong *et al.*<sup>15</sup> reported the occurrence of the D-center in the extended diffusion tail. According to early studies of the donor-acceptor pair recombination<sup>45</sup> the deep acceptor, which should be related to the D-center, was correlated with a boron defect on the carbon sublattice. Later the center was reinterpreted<sup>9,38,46</sup> as a complex of substitutional boron and a carbon vacancy. This interpretation is, however, not consistent with the ionization levels of the complexes  $B_C-V_C$  or  $B_{Si}-V_C$  obtained from first principles calculations<sup>7,32</sup> that are located in the upper half of the band gap. Other candidates including  $B_C$  and boron-antisite complexes were discussed.<sup>7,32</sup> The most promising candidate,<sup>7</sup> however, seems to be  $B_C$ . Yet, the limited accuracy of the calculated ionization levels does not permit a final conclusion. However, this identification could also explain the dependence of the deep acceptor concentration on the C/Si-ratio in CVD grown SiC.<sup>44</sup> It would also be consistent with the kinetic formation of  $B_C$  in the diffusion tails.

#### E. In-diffusion and the occurrence of diffusion zones

The in-diffusion experiments in 6H-SiC of Mokhov *et al.*<sup>9</sup> and Gao *et al.*<sup>44</sup> yielded boron profiles with two different zones at high surface concentrations of  $10^{20}$  cm<sup>-3</sup>. The first zone close to the surface contains a high boron concentration

and the more extended second zone a lower concentration. The appearance of two diffusion zones in the in-diffused boron profiles requires a more elaborate analysis that has to include, besides the bulk diffusion, also the surface reactions. However, two aspects we described above are certainly relevant, namely the trapping of  $B_{Hex}$  by  $B_{Si}$  in regions with a high boron concentration and the selective kick-out process of carbon split-interstitials.

### VIII. SUMMARY AND CONCLUSION

We investigate the role of silicon and carbon interstitials in the interstitial-mediated boron diffusion using an *ab initio* method. The migration path of the most stable boron interstitials, boron-vacancy complexes, and the kick-out reactions that initiate the interstitial-mediated boron diffusion are studied by a saddle point search method. The analysis of the interstitial-mechanisms for various doping conditions shows that three types of boron interstitials are relevant for the interstitial-mediated diffusion. For a moderately doped material we find that the positive hexagonal boron interstitial is most important. In strongly *p*- and *n*-doped SiC, the tetrahedrally carbon-coordinated interstitial, and the  $\langle 110 \rangle$ -oriented boron-silicon split interstitial dominate. Generally, the boron interstitial favors a migration via metastable split interstitial sites, thus avoiding a direct path. This finding is in agreement with recent investigations (Refs. 18 and 19) that focus on the hexagonal interstitial.

We calculated activation energies for the different diffusion channels. The comparison of the energies shows that the boron equilibrium diffusion is governed by the interstitial-mediated mechanism and not by the vacancy-assisted diffusion. These findings are in agreement with the analysis of experiments on the equilibrium and chemical boron diffusion. In particular, we were able to reproduce the experimental activation energy of the equilibrium diffusion (Ref. 23). At these experimental conditions the diffusion is dominated by the positive hexagonal interstitial. This is in nice agreement with the Fermi-level effects observed experimentally by Mokhov *et al.* (Ref. 9).

Our results further corroborate the experimental evidence for a kick-out mechanism (Refs. 10–12), also with respect to the absence of Fermi-level effects for a low dopant concentration. The theoretical modeling of the kick-out mechanism so far included only the interaction of the shallow boron acceptor with a silicon interstitial. We extended the to-date theoretical picture by analyzing the different role of carbon and silicon interstitials in the diffusion of the two substitutional boron defects. The central result is that the kick-out reactions with silicon interstitials initiate the diffusion of boron on both sublattices, while carbon interstitials only mediate the diffusion of boron on the carbon sublattice. The kick-in process of boron interstitials favors (due to the lower barrier) the formation of boron on the carbon sublattice at the diffusion front. We also find that carbon antisites, e.g., formed by carbon coimplantation, can capture boron interstitials and form a stable boron-carbon split interstitial. This defect complex primarily dissociates into a substitutional boron and a carbon interstitial, thus binding boron to the silicon

sublattice. In an excess of carbon-interstitials boron hence becomes essentially immobile, as observed experimentally (Ref. 10). We further describe small boron-carbon interstitial complexes and a diboron split interstitial on the silicon sublattice. Either of these defects may reduce the boron migration, given a high concentration of carbon interstitials or boron, respectively. These kinetically driven effects together with a possible carbon aggregation may also contribute to the

observed suppression of transient enhanced boron diffusion upon carbon coimplantation (Ref. 10).

#### ACKNOWLEDGMENTS

Discussions with Dr. Bracht, Dr. Linnarsson, and Dr. Pensl are gratefully acknowledged. This work was supported by the DFG within the SiC Research Group.

- 
- <sup>1</sup>P. M. Fahey, P. B. Griffin, and J. D. Plummer, *Rev. Mod. Phys.* **61**, 289 (1989).
- <sup>2</sup>S. Greulich-Weber, *Phys. Status Solidi A* **162**, 95 (1997).
- <sup>3</sup>H. Itoh, T. Troffer, C. Peppermüller, and G. Pensl, *Appl. Phys. Lett.* **73**, 1427 (1998).
- <sup>4</sup>H. H. Woodbury and G. W. Ludwig, *Phys. Rev.* **124**, 1083 (1961).
- <sup>5</sup>S. Yamada and H. Kuwabara, in *Silicon Carbide* (University of South Carolina Press, Columbia, SC, 1974), p. 305.
- <sup>6</sup>A. Fukumoto, *Phys. Rev. B* **53**, 4458 (1996).
- <sup>7</sup>M. Bockstedte, A. Mattausch, and O. Pankratov, *Mater. Sci. Forum* **353–356**, 447 (2001).
- <sup>8</sup>E. N. Mokhov, Y. A. Vodakov, G. A. Lomakina, V. G. Oding, G. F. Kholuyanov, and V. V. Semenov, *Fiz. Tekh. Poluprovodn. (S.-Peterburg)* **6**, 482 (1972) [*Sov. Phys. Semicond.* **6**, 414 (1972)].
- <sup>9</sup>E. N. Mokhov, E. E. Goncharov, and G. G. Ryabova, *Fiz. Tekh. Poluprovodn. (S.-Peterburg)* **18**, 49 (1984) [*Sov. Phys. Semicond.* **18**, 27 (1984)].
- <sup>10</sup>M. Laube, G. Pensl, and H. Itoh, *Appl. Phys. Lett.* **74**, 2292 (1999).
- <sup>11</sup>A. O. Konstantinov, *Fiz. Tekh. Poluprovodn. (S.-Peterburg)* **26**, 270 (1992) [*Sov. Phys. Semicond.* **26**, 151 (1992)].
- <sup>12</sup>H. Bracht, N. A. Stolwijk, M. Laube, and G. Pensl, *Appl. Phys. Lett.* **77**, 3188 (2000).
- <sup>13</sup>M. S. Janson, M. K. Linnarsson, A. Hallén, B. G. Svensson, N. Nordell, and H. Bleichner, *Appl. Phys. Lett.* **76**, 1434 (2000).
- <sup>14</sup>H. Itoh, T. Troffer, and G. Pensl, *Mater. Sci. Forum* **264–268**, 685 (1998).
- <sup>15</sup>M. Gong, C. V. Reddy, C. D. Beling, S. Fung, G. Brauer, H. Wirth, and W. Skorupa, *Appl. Phys. Lett.* **72**, 2739 (1998).
- <sup>16</sup>Y. Gao, S. I. Soloviev, and T. S. Sudarshan, *Appl. Phys. Lett.* **83**, 905 (2003).
- <sup>17</sup>M. Bockstedte and O. Pankratov, *Mater. Sci. Forum* **338–342**, 949 (2000).
- <sup>18</sup>R. Rurali, P. Godignon, J. Rebollo, P. Ordejón, and E. Hernández, *Appl. Phys. Lett.* **81**, 2989 (2002).
- <sup>19</sup>R. Rurali, E. Hernández, P. Godignon, J. Rebollo, and P. Ordejón, *Phys. Rev. B* **69**, 125203 (2004).
- <sup>20</sup>W. Windl, M. M. Bunea, R. Stumpf, S. T. Dunham, and M. P. Masquelier, *Phys. Rev. Lett.* **83**, 4345 (1999).
- <sup>21</sup>B. Sadigh, T. J. Lenosky, S. K. Theiss, M. J. Caturla, T. Diaz de la Rubia, and M. A. Foad, *Phys. Rev. Lett.* **83**, 4341 (1999).
- <sup>22</sup>P. Alippi, L. Colombo, P. Ruggerone, A. Sieck, G. Seifert, and T. Frauenheim, *Phys. Rev. B* **64**, 075207 (2001).
- <sup>23</sup>E. N. Mokhov, E. E. Goncharov, and G. G. Ryabova, *Fiz. Tverd. Tela (Leningrad)* **30**, 251 (1988) [*Sov. Phys. Solid State* **30**, 140 (1988)].
- <sup>24</sup>M. Bockstedte, A. Kley, J. Neugebauer, and M. Scheffler, *Comput. Phys. Commun.* **200**, 107 (1997).
- <sup>25</sup>M. Fuchs and M. Scheffler, *Comput. Phys. Commun.* **119**, 67 (1999).
- <sup>26</sup>H. J. Monkhorst and J. D. Pack, *Phys. Rev. B* **13**, 5188 (1976).
- <sup>27</sup>M. Bockstedte, A. Mattausch, and O. Pankratov, *Phys. Rev. B* **68**, 205201 (2003).
- <sup>28</sup>S. Lee, D. M. Bylander, and L. Kleinman, *Phys. Rev. B* **42**, 1316 (1990).
- <sup>29</sup>G. Wellenhofer and U. Rössler, *Phys. Status Solidi B* **202**, 107 (1997).
- <sup>30</sup>G. Makov and M. C. Payne, *Phys. Rev. B* **51**, 4014 (1995).
- <sup>31</sup>I. V. Ionova and E. A. Carter, *J. Chem. Phys.* **98**, 6377 (1993).
- <sup>32</sup>B. Aradi, A. Gali, P. Deák, E. Rauls, T. Frauenheim, and N. T. Son, *Mater. Sci. Forum* **353–356**, 455 (2001).
- <sup>33</sup>M. Bockstedte, A. Mattausch, and O. Pankratov, *Phys. Rev. B* **69**, 235202 (2004).
- <sup>34</sup>A. Mattausch, M. Bockstedte, and O. Pankratov, *Physica B* **308–310**, 656 (2001).
- <sup>35</sup>A. Gali, P. Deák, N. T. Son, and E. Janzén, *Mater. Sci. Forum* **389–393**, 477 (2002).
- <sup>36</sup>A. Gali, P. Deák, P. Ordejón, N. T. Son, E. Janzén, and W. J. Choyke, *Phys. Rev. B* **68**, 125201 (2003).
- <sup>37</sup>A. Mattausch, M. Bockstedte, and O. Pankratov, *Phys. Rev. B* **69**, 045322 (2004).
- <sup>38</sup>A. Gali, P. Deák, R. P. Devaty, and W. J. Choyke, *Phys. Rev. B* **60**, 10 620 (1999).
- <sup>39</sup>A. Zywiec, J. Furthmüller, and F. Bechstedt, *Phys. Rev. B* **59**, 15 166 (1999).
- <sup>40</sup>L. Torpo, M. Marlo, T. E. M. Staab, and R. M. Nieminen, *J. Phys.: Condens. Matter* **13**, 6203 (2001).
- <sup>41</sup>E. Rauls, T. Lingner, Z. Hajnal, S. Greulich-Weber, T. Frauenheim, and J.-M. Spaeth, *Phys. Status Solidi B* **217**, R1 (2000).
- <sup>42</sup>J. A. Van Vechten, *J. Phys. C* **17**, L933 (1984).
- <sup>43</sup>O. Pankratov, H. Huang, T. Diaz de la Rubia, and C. Mailhiot, *Phys. Rev. B* **56**, 13 172 (1997).
- <sup>44</sup>S. G. Sridhara, D. G. Nizhner, R. P. Devaty, W. J. Choyke, T. Troffer, G. Pensl, D. J. Larkin, and H. S. Kong, *Mater. Sci. Forum* **264–268**, 461 (1998).
- <sup>45</sup>H. Kuwabara and S. Yamada, *Phys. Status Solidi A* **30**, 739 (1975); H. Kuwabara, S. Shiokawa, and S. Yamada, *ibid.* **16**, K67 (1973).
- <sup>46</sup>A. van Duijn-Arnold, T. Ikoma, O. G. Poluektov, P. G. Baranov, E. N. Mokhov, and J. Schmidt, *Phys. Rev. B* **57**, 1607 (1998).